



## Electrochemical Performance of Tellurium Oxide on TiO<sub>2</sub>/Ti Array for Photoelectrocatalytic Chemical Oxygen Demand Sensor Applications

Maulidiyah<sup>1</sup>, Irwan<sup>2</sup>, Annisa Indriani<sup>1</sup>, La Ode Agus Salim<sup>3</sup>, Zul Arham<sup>4</sup>, Catherina M. Bijang<sup>5</sup>, Kurniawan Kurniawan<sup>6</sup>, and Muhammad Nurdin<sup>1\*</sup>

<sup>1</sup>Department of Chemistry, Universitas Halu Oleo, Kendari 93232, Indonesia

<sup>2</sup>Department of Pharmacy, Institut Teknologi Dan Kesehatan Avicenna, Kendari 93117, Indonesia

<sup>3</sup>Department of Chemistry, Institut Sains Teknologi dan Kesehatan (ISTEK) 'Aisyiyah Kendari, Kendari 93116, Indonesia

<sup>4</sup>Department of Mathematics and Natural Sciences, Institute Agama Islam Negeri (IAIN), Kendari 93563, Indonesia

<sup>5</sup>Department of Chemistry, Pattimura University, Ambon 97233, Indonesia

<sup>6</sup>Department of Textile Chemistry, Politeknik STTT Bandung, Bandung 40272, Indonesia

\*E-mail: mnurdin06@yahoo.com

### Article History

Received: 22 August 2021; Received in Revision: 13 December; Accepted: 20 December 2022

### Abstract

The experiments were carried out using Te-TiO<sub>2</sub>/Ti as working electrodes, prepared by the simple anodization technique and dip coating method, on Ti substrates (TiO<sub>2</sub>/Ti). The measurements were performed in an electrochemical cell using a three-electrode system, with Te-TiO<sub>2</sub>/Ti as the working electrode, Ag/AgCl as the reference electrode and Pt as the auxiliary electrode. A flow system for determining the profile and photocurrent response of reactive orange 84 was developed using Linear Sweep Voltammetry (LSV) and Multi-Pulse Amperometry (MPA). The physicochemical properties of Te-TiO<sub>2</sub>/Ti electrodes have been studied using UV-vis DRS analysis techniques and compared with un-doped TiO<sub>2</sub>/Ti electrodes. The UV-vis DRS showed that the TiO<sub>2</sub>/Ti doped Te functionally decreases bandgap to 3.0 eV. The results showed that the photocurrent of reactive orange 84 was observed in the concentration range (1-5 µM), with a linear response between concentration and charge.

Keywords: Chemical Oxygen Demand, photoelectrocatalytic, reactive orange 84, sensor, Te-TiO<sub>2</sub>/Ti

### 1. Introduction

The presence of various organic matter and other substances in water bodies is one of the benchmarks for the level of pollution in an aquatic environment. Organic compounds are one of the most dominant pollutants, both in the pharmaceutical, agricultural, urban, etc. (Li et al., 2021; Spahr et al., 2020). The level of organic matter pollution in water bodies can be determined by analyzing COD and BOD which help by microorganisms, chemicals and others. COD is an important parameter in the determination of an organic matter, because of its high accuracy, fast analysis and easy standardization compared to Biochemical Oxygen Demand (BOD) (Abou-Taleb et al., 2021; Corbella et al., 2019). Additionally, BOD doesn't provide any indication of the oxidation state of the organic matter. Thus, COD is considered an important parameter to assess the level of organic matter pollution in the aquatic environment. Currently, various methods have been developed for accurate

and sensitive determination of Chemical Oxygen Demand (COD) values.

Determination of the COD value is needed to measure the oxygen demand for organic substances which is difficult to degrade by oxidation. However, the selection of methods that are accurate, effectively, faster, and environmentally friendly was still major a serious problem among researchers. Conventional standard methods for the determination of COD have been widely used, such as the potassium dichromate (K<sub>2</sub>Cr<sub>2</sub>O<sub>7</sub>) method (Avila-Rojas et al., 2018). However, this method has several disadvantages its application is limited, the process is long (2-4 hours), has low detection sensitivity, produces toxic reagents (Cr<sub>2</sub>O<sub>7</sub><sup>2-</sup> and HgSO<sub>4</sub>), and is expensive (Ag<sup>+</sup>) (Kishimoto & Okumura, 2018; Zhang et al., 2018).

In recent years, photoelectrocatalytic (PEC) determination of COD based on TiO<sub>2</sub> has attracted attention because it provides another technique with a strong oxidizing

ability and low recombination of photogenerated electrons and holes (Arham et al., 2016; Azis et al., 2017; Muzakkar, Umar, et al., 2019).  $\text{TiO}_2$  photocatalyst is a strong and most promising candidate because of its strong PEC oxidation power, non-toxicity, environmental friendliness and good stability when applied in the environment (Muzakkar, Nurdin, et al., 2019; Nurdin et al., 2016; Nurdin, Agus, et al., 2019; Nurdin, Prabowo, et al., 2019). In addition,  $\text{TiO}_2$  when irradiated with UV light can be excited to generate electrons and holes. This hole will produce hydroxyl radicals ( $\bullet\text{OH}$ ) when interacting with water molecules (Maulidiyah, Ritonga, et al., 2015; Maulidiyah, Widianingsih, et al., 2015; Nurdin, Azis, et al., 2018). These hydroxyl radicals are powerful oxidizing agents that will be utilized for the degradation of organic molecules.

Although  $\text{TiO}_2$  has many advantages, such as high oxidizing ability, its application in visible irradiation is still very limited. Caused  $\text{TiO}_2$  is only active by exposure to UV light with a wide band gap energy ( $E_g$ ) (for anatase 3.2 eV) (Natsir et al., 2021; Nurdin, Dali, et al., 2018; Nurdin, Maulidiyah, et al., 2018; Wibowo et al., 2020). Several strategies have been applied, including the addition of dopants with the expectation of reducing the energy band gap so that light absorption can be shifted to visible irradiation. The selection of suitable dopants is very important to expand the absorption area of the  $\text{TiO}_2$  photocatalyst and reduce the gap energy. We found that Tellurium (Te) is a suitable dopant for  $\text{TiO}_2$  photocatalyst because it has a small band gap energy (0.32 eV) and valence band (VB) and conduction band (CB) for charge separation of  $\text{TiO}_2$ . In Addition, Te has a large enough electronegativity value so it has the potential as an electron acceptor material for  $\text{TiO}_2$  (Kim et al., 2019; Mondal et al., 2021).

Preparation of the dopant layer into the surface of the  $\text{TiO}_2/\text{Ti}$  film is an important factor to improve the performance of the PEC system. The dip-coating technique has been developed for the preparation of semiconductor layers because of its low cost, simple process, good performance, and controllable coating thickness.

This study describes a PEC technique for COD determination using Te- $\text{TiO}_2/\text{Ti}$  nanocomposite electrodes which is accurate and sensitive. Tellurium-modified  $\text{TiO}_2/\text{Ti}$  electrodes (Te- $\text{TiO}_2/\text{Ti}$ ) were made by a simple sol-gel method and anodizing method. RO 84 dye was used as a model compound to see the accuracy of the method. Moreover, the optical

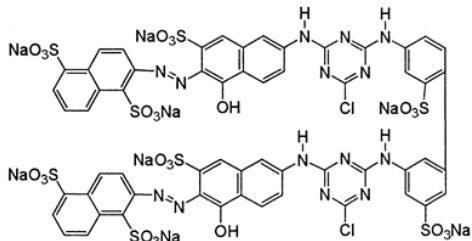
properties of the synthesized electrodes were also investigated.

## 2. Methodology

### 2.1. Materials

The materials used in this study were titanium plate (0.5 mm thick and 99% pure), titanium isopropoxide (> 97% pure), ethylene glycol ( $\text{C}_2\text{H}_6\text{O}_2$ ), telluric acid ( $\text{Te}(\text{OH})_6$ ) 99%, ammonium fluoride ( $\text{NH}_4\text{F}$ ), acid fluoride (HF), nitric acid ( $\text{HNO}_3$ ), sodium nitrate ( $\text{NaNO}_3$ ), glycerol 87%, plate copper (Cu) and reactive orange 84 (RO 84) dye was purchased from Sigma-Aldrich (M). The characteristics of the RO 84 dye are tabulated in Table 1.

**Table 1.** Properties of RO 84 dye.

Properties	Information
Common name	Reactive Orange 84
Molecular formula	$\text{C}_{58}\text{H}_{30}\text{Cl}_2\text{N}_{14}\text{Na}_8\text{O}_{26}\text{S}_8$
Molecular weight	1850.29
CAS registry number	91261-29-9
Molecular structure	

### 2.2. Preparation of $\text{TiO}_2/\text{Ti}$ plate

$\text{TiO}_2/\text{Ti}$  plate was used as the electrode substrate, and by cutting Ti Plate to a size of 4 x 0.5 cm and thickness of 0.5 mm. Then cleaned by soaking in a solution of HF,  $\text{HNO}_3$  and aquades in a ratio of 1:3:6 for 2 minutes in each solution. In the final stage,  $\text{TiO}_2/\text{Ti}$  plate was anodizing at a potential of 25 V in an electrolyte solution containing 87% glycerol, distilled water and 0.27 M  $\text{NH}_4\text{F}$ , the same as used in the previous work (Nurdin, Muzakkar, et al., 2022).

### 2.3. Synthesis of Te- $\text{TiO}_2/\text{Ti}$ nanocomposite electrodes

The- $\text{TiO}_2/\text{Ti}$  nanocomposite electrodes were prepared by the sol-gel and dip-coating method previously reported by (Bachvarova-Nedelcheva et al., 2016) with slight modifications. Firstly, solution A is made by mixing 8 mL of  $\text{Ti}[\text{OCH}(\text{CH}_3)_2]_4$  with 30 mL of  $\text{C}_2\text{H}_6\text{O}_2$ . Meanwhile, solution B was prepared by dissolving  $\text{Te}(\text{OH})_6$  into 30 mL of  $\text{C}_2\text{H}_6\text{O}_2$

with various concentrations of Te, 0.10%, 0.16%, 0.21% and 0.27%, respectively. Then the solution mixture was refluxed for 10 hours at 60°C. The Te-TiO<sub>2</sub> sol was evaporated at a temperature of 150°C to form a sol-gel. Furthermore, the prepared TiO<sub>2</sub>/Ti plate was coated with a Te-TiO<sub>2</sub> sol-gel using the dip-coating technique. The TiO<sub>2</sub>/Ti plate was immersed in the Te-TiO<sub>2</sub> sol-gel for 10 minutes and then slowly lifted vertically. After the coating process, the Te-TiO<sub>2</sub>/Ti electrode was calcined at 50°C for 10 minutes.

## 2.4. Experimental setup and procedures

All experiment was carried out in a reactor containing three-electrode such as Te-TiO<sub>2</sub>/Ti (working electrode), Ag/AgCl (reference electrode), and a platinum wire (counter electrode). The reactor structure has been reported in our previous paper (Nurdin et al., 2017). We used a xenon lamp with a power of 18 Watts and wavelength of 360 nm which is placed at the reactor near the working electrode and was used as the visible light source. 0.5 M NaNO<sub>3</sub> was chosen as the supporting electrolyte in this experiment. Reactive Orange 84 was used as the standard test compound for COD measurement studies along with various factors affecting COD measurement performance. RO 84 solution was prepared by dissolving RO 84 into distilled water, in which 0.1 M NaNO<sub>3</sub> was also added as a supporting electrolyte. About 10 mL of RO 84 solution was used in PEC reactions. The COD measurement was performed with a potentiostat portable (e-DY2100B).

## 3. Results and Discussion

### 3.1. UV-Vis DRS Analysis

To observe the optical properties of TiO<sub>2</sub>/Ti and Te-TiO<sub>2</sub>/Ti electrodes were analyzed using UV-Vis DRS spectrometry within the wavelength range of 250–550 nm. Figure 1 shows the difference in band gap energy between TiO<sub>2</sub>/Ti electrodes and Te-modified TiO<sub>2</sub>/Ti electrodes. TiO<sub>2</sub> film without the addition of dopants has a band gap energy of 3.25 eV. While the band gap energy of the Te-TiO<sub>2</sub>/Ti electrode is around 3.0 eV, this shows that the addition of tellurium can reduce the band gap energy of TiO<sub>2</sub> (He et al., 2018; Mathew et al., 2020). This phenomenon will reduce the energy required to activate the TiO<sub>2</sub> photocatalyst so that electrons will be more easily excited from the valence band to the conduction band. The more electrons in the conduction band, the greater the opportunity for the electron charge to reach the photocatalyst surface (Guo et al., 2020;

Hamdy et al., 2021). So that it has an impact on the maximum degradation process. In addition, the decrease in band gap energy also causes a shift in the absorption wavelength of the electrode to the visible region (400–800 nm) so that the degradation ability of the Te-TiO<sub>2</sub>/Ti electrode is more optimum. The UV-Vis DRS results informed that Te entering the TiO<sub>2</sub> atomic lattice can narrow the band gap energy, thereby shifting the absorption to the UV-Vis region which might improve the photoelectrocatalytic performance of the TiO<sub>2</sub> film.

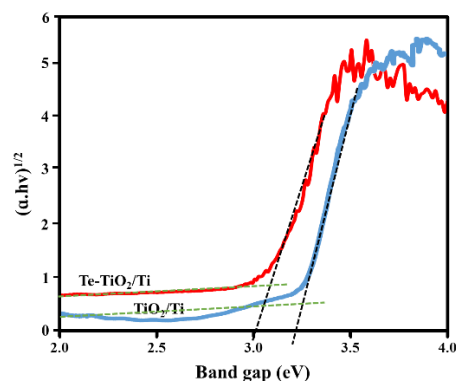


**Figure 1.** Bandgap spectra of TiO<sub>2</sub>/Ti compared with Te-TiO<sub>2</sub>/Ti electrode.

### 3.2. Linear Sweep Voltammetry of Te-TiO<sub>2</sub>/Ti electrode

LSV test was carried out to observe the electrochemical properties and also the current response in UV and visible irradiation toward the Te-TiO<sub>2</sub>/Ti electrode. The LSV test was carried out in the potential range of -1 Volt - 1 Volt with a scan rate of 0.05 V/s and a sensitivity of 1 × 10<sup>-4</sup> and 0.5 M NaNO<sub>3</sub> as a supporting electrolyte (Nurdin, Wibowo, et al., 2022). Figure 2A shows that the Te-TiO<sub>2</sub>/Ti electrodes with variations concentrations of Te of 0.10%, 0.16% and 0.21% respectively did not produce peak currents. This phenomenon was caused by the absence of a given light source to excite electrons (e<sup>-</sup>) on the surface of TiO<sub>2</sub> from the valence band (VB) to the conduction band (CB).

Under different conditions when exposed to UV and visible illumination (Figure 2B and 2C) the Te-TiO<sub>2</sub>/Ti electrodes showed a significant increase in current. Figure 2B shows the LSV plots of the different electrodes under UV light. Te-TiO<sub>2</sub>/Ti electrodes with various concentrations showed high photocurrent density. The highest photocurrent was achieved when the Te concentration of 0.1% compared to other concentrations. It was different when the Te-TiO<sub>2</sub>/Ti electrode was illumination to visible light, producing a

relatively weak current (Figure 2C). Although Te was able to reduce the band gap energy of  $\text{TiO}_2$  as evidenced by UV-Vis DRS data, its performance in the visible region is not effective.

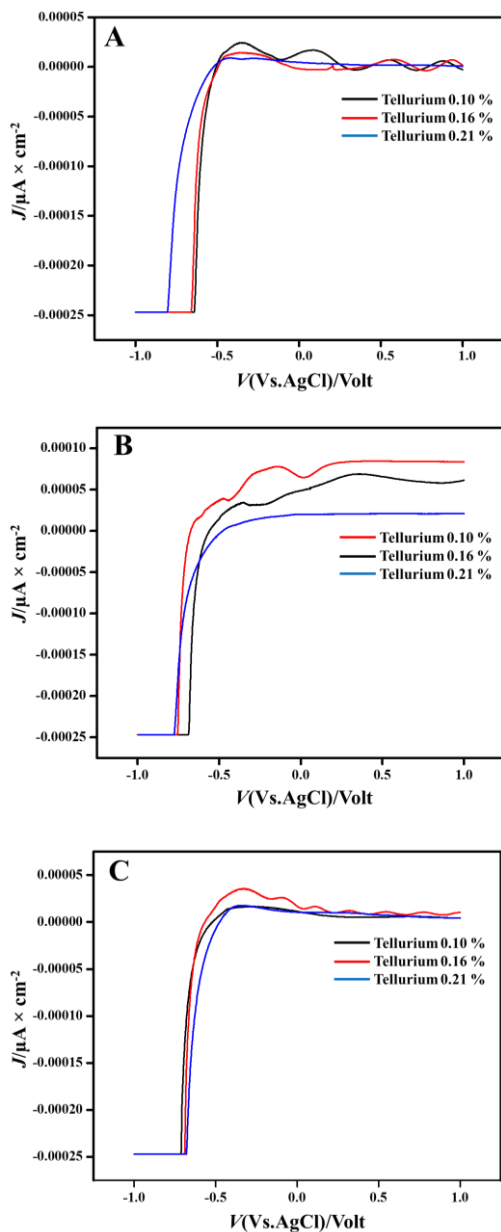


**Figure 2.** LSV voltammogram curves of (a) Te- $\text{TiO}_2/\text{Ti}$  electrode in the dark, (b) Te- $\text{TiO}_2/\text{Ti}$  electrode under UV illumination and, (c) Te- $\text{TiO}_2/\text{Ti}$  electrode under visible illumination. Electrolyte: 0.1 M  $\text{NaNO}_3$  solution.

It is clear that the difference in the light current response of the Te- $\text{TiO}_2/\text{Ti}$  electrodes in the dark and when exposed to UV light (Figure 2). In dark conditions, the anodic current response is seen to be close to zero, this indicates that the conductivity of the lightless electrode is very small. Unlike the

case with electrodes treated with UV light, the anodic current response increased with increasing potential. This phenomenon indicates that the Te- $\text{TiO}_2/\text{Ti}$  electrode becomes conductive.

### 3.3. Multi Pulse Amperometry of Te- $\text{TiO}_2/\text{Ti}$ electrode

Measurement of the photocurrent response of Reactive Orange 84 was carried out using the MPA technique. The experiment was carried out using a three-electrode system (Maulidiyah et al., 2017; Tribawono et al., 2016).

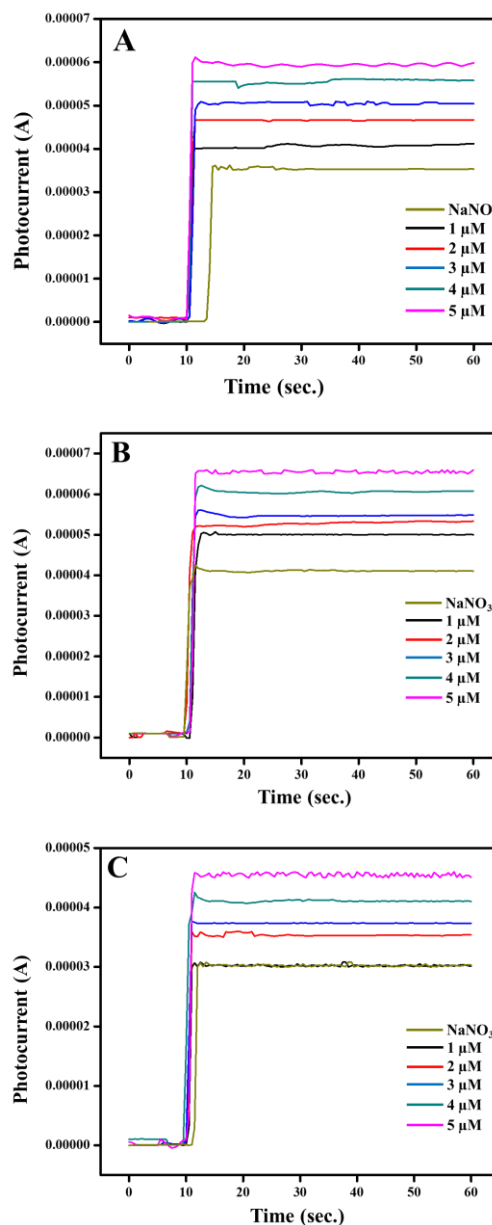


**Figure 3.** Amperogram of Te- $\text{TiO}_2/\text{Ti}$  electrodes against test compounds RO 84; (A) Te 0.10%, (B) 0.16%, and (C) Te 0.21%

The MPA test was carried out at a potential of 0.6 V, a sample time of 0.5 seconds and a running time of 60 seconds with 0.1 M  $\text{NaNO}_3$  (electrolyte solution). The choice of  $\text{NaNO}_3$  electrolyte solution in the PEC system is based on its ability to conduct electric current.

Based on Figure 3, it can be seen that the initial photocurrent increases with increasing solution concentration. The MPA response indicated that this compound was well degraded by the  $\text{Te-TiO}_2/\text{Ti}$  electrode. In Figure 3C, it can be seen that the current RO 84 coincides with the current of the  $\text{NaNO}_3$  electrolyte solution. This phenomenon indicates that RO 84 has been completely degraded by the electrodes.

Figure 4 confirmed that the charge (Q) of RO 84 increases as the concentration of the solution increases. The value of the light current increases linearly with increasing concentration. This is in accordance with Faraday's law that the value of charge is proportional to concentration,  $Q = nFVC$  (Priya & Jeyanthi, 2019; Zini et al., 2020). Overall, the three electrodes showed good performance, this is evidenced by the charge value from the measurement results close to the theoretical charge value (Nurdin, Muzakkar, et al., 2022). The electrode with 0.16% Te concentration is the electrode that has a charge value that is closest to the theoretical charge value of the test sample.

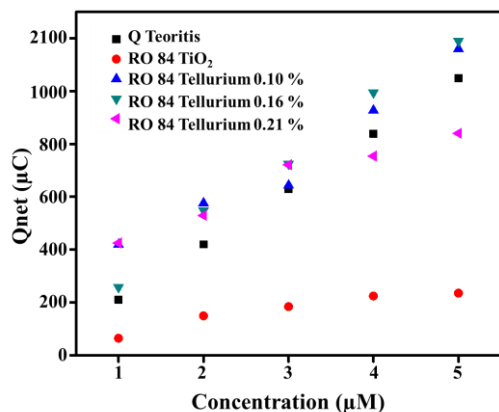


**Figure 4.** The relationship between  $Q_{\text{net}}$  and the concentrations of RO 84 dye.

### 3.4. Determination of COD Value

Figure 5 shows the relevant correlations between the photocurrent and the different RO 84 concentrations, computed as COD values. The photocurrent generated from each measurement of the COD value is subtracted from the current value of the blank solution, to obtain the net current value ( $Q_{\text{net}}$ ).

In this part, the  $\text{Te-TiO}_2/\text{Ti}$  electrode was used to measure the COD of RO 84 solutions. As can be seen from Figure 5, as the COD value increases, the I value increases. In addition, the graph shows that the net current value is highest when the tellurium concentration of 0.16%, while the current value is lowest when the tellurium concentration of 0.21%. This is primarily during the reaction process, a large quantity of OH radicals were produced which oxidized the dye RO 84. This demonstrated the different catalytic degradation capabilities of the three-electrode, owing to the different concentrations of tellurium. It can be observed that for all the electrodes investigated, the number of net loads obtained is directly proportional to the concentration.

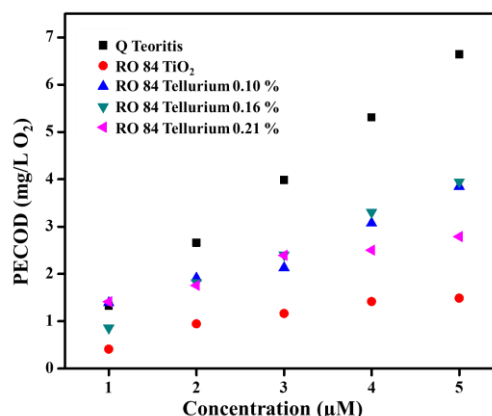


**Figure 5.** The relationship between PECOD and the concentrations of RO 84 dye.

## 4. Conclusion

In this work, the influence concentration of tellurium on the  $\text{TiO}_2/\text{Ti}$  electrode for assessing COD has been investigated. In short,  $\text{Te-TiO}_2/\text{Ti}$  electrode was prepared by the electrochemical anodization method. The photoelectrochemical properties of the electrode were examined, indicating that the Te dopant can facilitate the transfer of electrons  $\text{TiO}_2/\text{Ti}$  electrode, which is favorable to advancing photocatalytic performance for oxidation of the RO 84 dye. The experimental results LSV and MPA exhibited that  $\text{Te-TiO}_2/\text{Ti}$  showed high activity and good stability for PEC. We also found that the  $\text{Te-TiO}_2/\text{Ti}$  electrode produced a photocurrent which is linearly correlated with the dye concentration RO 84 during photoelectrocatalytic degradation.

## Acknowledgement

We acknowledge the financial support from the Ministry of Education, Culture, Research and Technology of the Republic of Indonesia

under the basic research award grant no. 51/UN29.20/PG/2022.

## References

- Abou-Taleb, E. M., Hellal, M. S., & Kamal, K. H. (2021). Electro-oxidation of phenol in petroleum wastewater using a novel pilot-scale electrochemical cell with graphite and stainless-steel electrodes. *Water Environ J.* 35(1), 259–268. <http://dx.doi.org/10.1111/wej.12624>
- Arham, Z., Nurdin, M., & Buchari, B. (2016). Photoelectrocatalysis Performance of  $\text{La}_2\text{O}_3$  doped  $\text{TiO}_2/\text{Ti}$  Electrode in Degradation of Rhodamine B Organic Compound. *Int J ChemTech Res.* 9(11), 113–120.
- Avila-Rojas, S. H., Tapia, E., Briones-Herrera, A., Aparicio-Trejo, O. E., León-Contreras, J. C., Hernández-Pando, R., & Pedraza-Chaverri, J. (2018). Curcumin prevents potassium dichromate ( $\text{K}_2\text{Cr}_2\text{O}_7$ )-induced renal hypoxia. *Food Chem. Toxicol.* 121, 472–482. <https://doi.org/10.1016/j.fct.2018.09.046>
- Azis, T., Nurwahidah, A. T., Wibowo, D., & Nurdin, M. (2017). Photoelectrocatalyst of Fe co-doped N- $\text{TiO}_2/\text{Ti}$  nanotubes: Pesticide degradation of thiamethoxam under UV-visible lights. *Environ. Nanotechnol. Monit. Manag.* 8, 103–111. <https://doi.org/10.1016/j.enmm.2017.06.002>
- Bachvarova-Nedelcheva, A., Iordanova, R., Gegova, R., & Dimitriev, Y. (2016). Sol-gel synthesis, characterization and optical properties of  $\text{TiO}_2/\text{TeO}_2$  powders. *Bulg. Chem. Commun.* 48, 5–10.
- Corbella, C., Hartl, M., Fernandez-gatell, M., & Puigagut, J. (2019). MFC-based biosensor for domestic wastewater COD assessment in constructed wetlands. *Sci. Total Environ.* 660, 218–226. <https://doi.org/10.1016/j.scitotenv.2018.12.347>
- Guo, Y., Nan, J., Xu, Y., Cui, F., Shi, W., & Zhu, Y. (2020). Thermodynamic and dynamic dual regulation  $\text{Bi}_2\text{O}_3\text{CO}_3/\text{Bi}_5\text{O}_7\text{I}$  enabling high-flux photogenerated charge migration for enhanced visible-light-driven photocatalysis. *J. Mater. Chem. A.* 8(20), 10252–10259. <https://doi.org/10.1039/D0TA02588G>
- Hamdy, M. S., Abd-Rabboh, H. S. M., Benaissa, M., Al-Metwaly, M. G., Galal, A. H., & Ahmed, M. A. (2021). Fabrication of novel polyaniline/ $\text{ZnO}$  heterojunction for exceptional photocatalytic hydrogen production and degradation of fluorescein dye through direct Z-scheme mechanism. *Opt. Mater.* 117, 1–13. <https://doi.org/10.1016/j.optmat.2021.111198>
- He, H., Peng, X., Yu, Y., Shi, Z., Xu, M., Ni, S., & Gao, Y. (2018). Photochemical vapor generation of tellurium: synergistic effect from ferric ion and nano- $\text{TiO}_2$ . *Anal. Chem.* 90(9), 5737–5743. <https://doi.org/10.1021/acs.analchem.8b00022>
- Kim, C., Lopez, D. H., Kim, D. H., & Kim, H. (2019). Dual defect system of tellurium antisites and silver interstitials in off-stoichiometric  $\text{Bi}_2(\text{Te},\text{Se})_{3+y}$  causing enhanced thermoelectric performance. *J. Mater. Chem. A.* 7(2), 791–800. <https://doi.org/10.1039/C8TA05261A>
- Kishimoto, N., & Okumura, M. (2018). Feasibility of mercury-free chemical oxygen demand (COD) test with excessive addition of silver sulfate. *J. Water Environ. Technol.* 16(6), 221–232. <http://dx.doi.org/10.2965/jwet.18-016>
- Li, Q., Chen, Z., Wang, H., Yang, H., Wen, T., Wang, S., Hu, B., & Wang, X. (2021). Removal of organic compounds by nanoscale zero-valent iron and its composites. *Sci. Total Environ.* 792, 1–17. <https://doi.org/10.1016/j.scitotenv.2021.148546>
- Mathew, S., Ganguly, P., Kumaravel, V., Harrison, J., Hinder, S. J., Bartlett, J., & Pillai, S. C. (2020). Effect of chalcogens (S, Se, and Te) on the anatase phase stability and photocatalytic antimicrobial activity of  $\text{TiO}_2$ . *Mater. Today: Proc.* 33, 2458–2464. <https://doi.org/10.1016/j.matpr.2020.01.336>
- Maulidiyah, M., Wibowo, D., Herlin, H., Andarini, M., Ruslan, R., & Nurdin, M. (2017). Plasmon enhanced by Ag-doped S- $\text{TiO}_2/\text{Ti}$  electrode as highly effective photoelectrocatalyst for degradation of methylene blue. *Asian J. Chem.* 29, 2504–2508.

- <http://dx.doi.org/10.14233/ajchem.2017.20836>
- Maulidiyah, M., Widianingsih, E., Azis, T., & Wibowo, D. (2015). Preparation of visible photocatalyst N-TiO<sub>2</sub> and its activity on Congo red degradation. *ARNP J. Eng. Appl. Sci.* 10(15), 6250–6256.
- Maulidiyah, Ritonga, H., Faiqoh, C. E., Wibowo, D., & Nurdin, M. (2015). Preparation of TiO<sub>2</sub>-PEG thin film on hydrophilicity performance and photocurrent response. *Biosci. Biotechnol. Res. Asia.* 12(3), 1985–1989.  
<https://doi.org/10.13005/bbra/1865>
- Mondal, R., Biswas, D., Paul, S., Das, A. S., Chakrabarti, C., Roy, D., Bhattacharya, S., & Kabi, S. (2021). Investigation of microstructural, optical, physical properties and dielectric relaxation process of sulphur incorporated selenium–tellurium ternary glassy systems. *Mater. Chem. Phys.* 257, 1–14.  
<https://doi.org/10.1016/j.matchemphys.2020.123793>
- Muzakkar, M. Z., Nurdin, M., Ismail, I., Maulidiyah, M., Wibowo, D., Ratna, R., Saad, S. K. M., & Umar, A. A. (2019). TiO<sub>2</sub> Coated-Asphalt Buton Photocatalyst for High-Performance Motor Vehicles Gas Emission Mitigation. *Emiss. Control Sci. Technol.* 6, 28–36.  
<https://doi.org/10.1007/s40825-019-00132-3>
- Muzakkar, M. Z., Umar, A. A., Ilham, I., Saputra, Z., Zulfikar, L., Maulidiyah, M., Wibowo, D., Ruslan, R., & Nurdin, M. (2019). Chalcogenide material as high photoelectrochemical performance Se doped TiO<sub>2</sub>/Ti electrode: Its application for Rhodamine B degradation. *J. Phys. Conf. Ser.* 1242(1), 12016.  
<http://dx.doi.org/10.1088/1742-6596/1242/1/012016>
- Natsir, M., Putri, Y. I., Wibowo, D., Maulidiyah, M., Azis, T., Bijang, C. M., Mustapa, F., Irwan, I., Arham, Z., & Nurdin, M. (2021). Effects of Ni-TiO<sub>2</sub> Pillared Clay-Montmorillonite Composites for Photocatalytic Enhancement Against Reactive Orange Under Visible Light. *J Inorg Organomet Polym.* 31, 3378–3388.  
<https://doi.org/10.1007/s10904-021-01980-9>
- Nurdin, M., Agus, L., Putra, A. A. M., Maulidiyah, M., Arham, Z., Wibowo, D., Muzakkar, M. Z., & Umar, A. A. (2019). Synthesis and electrochemical performance of graphene-TiO<sub>2</sub>-carbon paste nanocomposites electrode in phenol detection. *J. Phys. Chem. Solids.* 131, 104–110.  
<https://doi.org/10.1016/j.jpcs.2019.03.014>
- Nurdin, M., Azis, T., Maulidiyah, M., Aladin, A., Hafid, N. A., Salim, L. O. A., & Wibowo, D. (2018). Photocurrent Responses of Metanil Yellow and Remazol Red B Organic Dyes by Using TiO<sub>2</sub>/Ti Electrode. *IOP Conf. Ser.: Mater. Sci. Eng.* 367(1), 12048.  
<http://dx.doi.org/10.1088/1757-899X/367/1/012048>
- Nurdin, M., Dali, N., Irwan, I., Maulidiyah, M., Arham, Z., Ruslan, R., Hamzah, B., Sarjuna, S., & Wibowo, D. (2018). Selectivity Determination of Pb<sub>2+</sub> Ion Based on TiO<sub>2</sub>-Ionophores BEK6 as Carbon Paste Electrode Composite. *Anal. Bioanal. Electrochem.* 10(12), 1538–1547.
- Nurdin, M., Maulidiyah, M., Salim, L. O. A., Muzakkar, M. Z., & Umar, A. A. (2018). High performance cypermethrin pesticide detection using anatase TiO<sub>2</sub>-carbon paste nanocomposites electrode. *Microchem. J.* 14, 756–761.  
<https://doi.org/10.1016/j.microc.2018.11.050>
- Nurdin, M., Muzakkar, M. Z., Maulidiyah, M., Maulidiyah, N., & Wibowo, D. (2016). Plasmonic Silver–N/TiO<sub>2</sub> Effect on Photoelectrocatalytic Oxidation Reaction. *J Mater Env. Sci.* 7(9), 3334–3343.
- Nurdin, M., Muzakkar, M. Z., Maulidiyah, M., Trisna, T., Arham, Z., La Salim, O. A., Irwan, I., & Umar, A. A. (2022). High Performance COD Detection of Organic Compound Pollutants using Sulfurized TiO<sub>2</sub>/Ti Nanotube Array Photoelectrocatalyst. *Electrocatalysis* 13(5), 1–10.  
<http://dx.doi.org/10.1007/s12678-022-00746-2>
- Nurdin, M., Prabowo, O. A., Arham, Z., Wibowo, D., Maulidiyah, M., Saad, S. K. M., & Umar, A. A. (2019). Highly sensitive fipronil pesticide detection on ilmenite (FeO.TiO<sub>2</sub>)-carbon paste composite electrode. *Surf. Interfaces* 16, 108–113.

- <https://doi.org/10.1016/j.surfin.2019.05.008>
- Nurdin, M., Wibowo, D., Azis, T., Safitri, R. A., Maulidiyah, M., Mahmud, A., Mustapa, F., Ruslan, R., Salim, A., & Ode, L. (2022). Photoelectrocatalysis Response with Synthetic Mn-N-TiO<sub>2</sub>/Ti Electrode for Removal of Rhodamine B Dye. *Surf. Engin. Appl. Electrochem.* 58(2), 125-134.  
<https://doi.org/10.3103/S1068375522020077>
- Nurdin, M., Zaeni, A., Rammang, E. T., Maulidiyah, M., & Wibowo, D. (2017). Reactor design development of chemical oxygen demand flow system and its application. *Anal. Bioanal. Electrochem.* 9(4), 480-494.
- Priya, M., & Jeyanthi, J. (2019). Removal of COD, oil and grease from automobile wash water effluent using electrocoagulation technique. *Microchem. J.* 150, 1-8.  
<https://doi.org/10.1016/j.microc.2019.104070>
- Spahr, S., Teixidó, M., Sedlak, D. L., & Luthy, R. G. (2020). Hydrophilic trace organic contaminants in urban stormwater: Occurrence, toxicological relevance, and the need to enhance green stormwater infrastructure. *Environ. Sci. Water Res. Technol.* 6(1), 15-44.
- <https://doi.org/10.1039/C9EW00674E>
- Tribawono, D. S., Wibowo, D., & Nurdin, M. (2016). Electrochemical profile degradation of amino acid by flow system using TiO<sub>2</sub>/Ti nanotubes electrode. *Anal. Bioanal. Electrochem.* 8(6), 761-776.
- Wibowo, D., Sufandy, Y., Irwan, I., Azis, T., Maulidiyah, M., & Nurdin, M. (2020). Investigation of nickel slag waste as a modifier on graphene-TiO<sub>2</sub> microstructure for sensing phenolic compound. *J. Mater Sci: Mater Electron.* 3, 14375-14383.  
<https://doi.org/10.1007/s10854-020-03996-2>
- Zhang, S., Chen, W., Liu, Y., Luo, P., & Gu, H. (2018). A Modified Method for the Accurate Determination of Chemical Oxygen Demand (COD) in High Chloride Oilfield Wastewater. *OJOGas* 3(4), 263-277.  
<https://doi.org/10.4236/ojogas.2018.34023>
- Zini, L. P., Longhi, M., Jonko, E., & Giovanela, M. (2020). Treatment of automotive industry wastewater by electrocoagulation using commercial aluminum electrodes. *Process Saf. Environ. Prot.* 142, 272-284.  
<https://doi.org/10.1016/j.psep.2020.06.029>